Enhancement of physical and chemical properties of halloysite nanotubes using sulfuric acid

Tayser Sumer Gaaz[1,2]*, Abu Bakar Sulong[1], Abdul Amir H. Kadhum[3], Muneer Ba-Abbad[3] and Ahmed A. Al-Amiery [3]*.

1 Department of Mechanical & Materials Engineering, Faculty of Engineering & Built Environment, Universiti Kebangsaan Malaysia; E-Mail: taysersumer@gmail.com (T.S.G); abubakar@eng.ukm.my (A.B.S);

2 Department of Equipment's & Machines Engineering, Technical College Al-Musaib, Al-Furat Al-Awsat Technical University, Iraq.

3 Department of chemical & Process Engineering, Faculty of Engineering & Built Environment, Universiti Kebangsaan Malaysia; E-Mail: amir@eng.ukm.my (A.H.K); muneer711@gmail.com (M.M.B).

* Author to whom correspondence should be addressed; E-Mail: taysersumer@gmail.com; and abubakar@eng.ukm.my.
Tel.: +6-011-282-91774.

The research is financed by: The authors thank Universiti Kebangsaan Malaysia and the Ministry of Higher Education for the financial support grand DIP-2014-006 and LRGS/TD/2012/USM-UKM/PT/05.

Abstract: Investigates the enhancement of physical and chemical properties of natural nanotubes halloysite (HNTs) that has chemical formula of $Al_2Si_2O_5(OH)_4$ are unique and versatile using sulfuric acid at various experimental conditions. The findings obtained from the use of Fourier transform infrared spectroscopy (FT-IR) reveal that acid breaks down the crystal structure of HNTs before it changes into amorphous silica. Another finding reveals that X-ray diffraction (XRD) causes the H_2SO_4 to break down the crystal structure of HNTs and to charge into the structure amorphous silica. The reaction of the acid with both the outer and inner surfaces of the nanotubes causes the AlO_6 octahedral layers to dissolve, which then leads to the break down and collapse of the tetrahedral layers of SiO_4. The final product from this treatment is treated HNTs H_2SO_4 with characteristics for commercial use fixed micropore size distribution and as effective low-cost adsorbents. The maximum adsorption capacity for methylene blue is greater than 60 mgg−1 and the pH value can be used to control the adsorption capacity. Also, this treatment has been potentially identified for use in the production of biomedical applications.

Keywords: nanotubes; Pore size; Surface area

1. Introduction

Halloysite nanotubes (HNTs) are a compound that consists mainly of aluminosilicate nanoclay mineral with natural nanotubular structure. Generally, the stoichiometry of HNT is noted as $Al_2O_3 \cdot 2SiO_2 \cdot nH_2O$, whereby n is 2 for halloysite-(7 Å) and n is 4 for halloysite-(10 Å). The basal (d001) spacing for halloysite-(7 Å) and kaolinite (7 Å) is the same. However the basal (d001) spacing (7 Å) is lower than that of hydrated halloysite-(10 Å). This is because the interlayer water in halloysite-(10 Å) evaporates easily in dry air; resulting in halloysite-(7 Å). The crystal structure of HNT consists of two layers. The structure is formed by a corner sharing SiO4 tetrahedral layer and an edge sharing AlO6 octahedral layer. These two layers are separated by a single layer of interlayer water molecules [1-3]. Generally, HNT is used widely in a range of applications in numerous areas used in thermoplastic, plastic, polymer and other composites as additive fillers. Also its hollow nanotubular structure has made it a potential substance for use in the production of biomedical applications [4]. However, the interlayer water often causes mismatch of tetrahedral layer and octahedral layer. This causes charges in chemical and physical properties of HNT such as cation exchange capacity [4-6]. As a nanoclay mineral, halloysite is used in the production of high quality porcelain products [7]. A team of researchers, Zhang et al. examined the effects of sulfuric acid (H_2SO_4) and alkaline activation on kaolinite. Their findings showed that H_2SO_4 activation with 6 M HCl and under reflux conditions of 6 hours experience the removal of about 90% of the octahedral Al_3+ cations, resulting in amorphous silica with high surface area. One of the differences lies in the regular crystal structure of Kaolinite that requires pre-heating preparation for its reaction with H_2SO_4 [8]. The H_2SO_4 treatment a traditional chemical activation method is an efficient approach for the improvement of the performance of nanoclay minerals [9-11]. The H_2SO_4 treatment triggers several processes; disaggregation of nanoclay particles, elimination of mineral impurities, and dissolution of the external layers. These processes break down, the structure of clay minerals, resulting in an increase in surface activity, BET specific surface area [8, 12]. Meanwhile Panda et al. [12] investigated the enhancement of physical and chemical characteristics of kaolin using H2SO4 treatment. They studied the use of H_2SO_4 treatment as an effective process for manufacturing active surfaces and porous materials with high surface area [12]. The physical characteristic of HNT particles measure 50 to 70 nm in external diameter, 15 nm in diameter lumen and 1 ± 0.5 μm in length. One important characteristics of HNTs are the chemistry of the outer and inner surfaces are different, hence these two surfaces have separate modifications [13]. There are a number of researches suggested on H_2SO_4 treatment of Kaolinite-the isomeric mineral of HNT. One of the studies by Lenarda et al. used H_2SO_4 treatment on meta-

kaolin for the preparation of mesoporous catalysts [14]. Yet there are deficiencies in HNT. For one, there is mismatching of the tetrahedral layer and octahedral layer due to interlayer water. When this happens, there is a direct reduction with acid. Secondly, HNT reacts with acid easily due to its nanotubular structure in contrast with kaolinite that does not react with acid easing due to kaolinite its plate structure [15]. Like HNT, kaolinite too benefits from H2SO4 treatment in terms of increased surface area, higher porosity level and more number of H2SO4 centers [16-19]. Various methods such as acid-activation, intercalation, thermal-chemical treatment and chemical modification are employed in the functionalization of HNT. All these methods have improved the properties of HNT as well as the performances of related products. Hence, HNT has attracted considerable interests among the stake holders. It is clear that acid treatment causes disaggregation of HNT and even the dissolution of the inner layers. In a recent study by Wang et al., the used of H_2SO_4 for selective etching of alumina from the inner wall could enlarge the lumen of HNT [20]. As such, this study, presents the systematic investigation of processes using H2SO4 in the acid treatment of HNT. This is followed by an examination of the effects of H_2SO4 treatment on the morphology, structure, and porous characteristics of HNT by the analysis of TG–DTA, XRD, and BET. The findings revealed that the crystal structure of HNT was broken down but the surface area of BET and pore volume was enhanced by H_2SO_4 treatment. In addition, the investigation of the adsorption behavior of H_2SO_4 treatment HNT for methylene blue (MB) indicated a key role the pH value plays in the adsorption process of MB.

2. Experimental Section

2.1. Materials

The main materials used for this experiment are sulfuric acid (ACS reagent, 95-98% H_2SO_4), which was supplied by Sigma Aldrich and Halloysite Nanotubes (HNT) which were purchased from Natural Nano, New York. Tables land 2 show chemical compositions of HNT and the analysis of the physical properties of HNTs. All the materials used are in their original form, without any further purification.

Table 1

Table 2

3.1.1. Procedures in acid treatment of Halloysite Nanotubes

The following is a description of the procedures involved in the acid treatment of Halloysite Nanotubes (HNTs). The first step is to add 15 g of HNT into 100 mL of 3 M H_2SO_4 solution which is of mol L^{-1} concentration. After that, the mixture was placed in to a water bath kept at a maintained temperature of 90º C and under a stirring speed 200 of rpm for varying time duration 1

h, 3 h, 8 h and 21 h. Then, the mixtures are separated using a centrifuge speed of 3000 rpm for 10 min. The purpose is to separate the pastel from the solution. The presented was next; the paste is washed using distilled water up to four times. This is followed by the drying process where log the paste is left in the oven at 70º C for 12 h. Finally dried HNTs were ground using a mortar. The samples were named H0, H1, H3, H8 and H21 based on duration of the treatment time of H_2SO_4 as in untreated (0 hr) 1, 3, 8 and 21 hr respectively.

3.2. Characteristics

3.2.1. *Fourier Transform Infrared Spectroscopic analysis (FTIR)*

The analysis of FTIR is to identify the characteristics of possible interaction of HNTs. The analysis is performed using Perkin Elmer System 2000 that is equipped with attenuated total reflectance (ATR). For this research work, the range for the FTIR spectrum has been set in the range of 650 to 4000 cm^{-1} with a 0.4 cm^{-1} resolution.

3.2.2. *X-ray diffraction (XRD)*

The analysis of XRD investigates the structure and crystallite size of HNTs. The equipment used to perform this analysis is form Germany. It is the XRD Diffractometer of model D8 with advance Bruker AXS X-ray and Cu Radiation 1.5406 Å. The EVA software (version 2) was used for the evaluation of the structure and lattice strain of samples. Finally, the XRD patterns of all the samples were wed to compare with the Joint Committee on Powder Diffraction Standards (JCPDS).

3.2.3. Thermogravimetric (TGA)

The analysis of Thermogravimetric is to identify the thermal properties of all specimens. The analysis is performed using the TGA Model Q600 of TA Instrument in New Castle, DE. First, the specimens are dried in an air circulating oven at 45 ºC for 12 hr before using them to conduct the tests. This is followed by the preparation of the physical conditions to perform the TGA tests. One of the conditions is to set the temperature between 25 ºC and 800 ºC in a nitrogen gas filled atmosphere where by flow rate of the gas is 60 ml/min. The other condition is the scanning rate is set at 10 ºC/min.

3.2.4. Morphology

The Field Emission Scanning Electron Microscope (FESEM) of model ZEISS SUPRA 55-VP is used to investigate and view the morphology of the HNTs samples. This model is equipped with a higher resolution and it has lower charging on the sample surface. The magnifications of the morphology observations are set at 10, 25, 50, 100 and 200 k. The elemental analysis of HNTs is performed using OXFORD EDS and Mapping.

3.2.5. BET surface area and pore volume

Bruncher-Emmett-Teller (BET) is a widely used isotherm technique. It is used by man to determine the surface area of the materials calculating the physical adsorption of nitrogen gas molecules. The analysis of the surface area of the samples was performed using a Gemini apparatus (Micromeritics ASAP 2020, GA, and USA). However, the reliability and accuracy of the instrument is ± 2% m^2/g. This is because silica alumina is used in the calibration. The measurement is based on Nitrogen adsorption isotherms process. The samples are subjected to the degassing process at 350 °C for 2 h under 50 mTorr of vacuum. The Barrett-Joyner-Halenda (HJH) equation obtained from the nitrogen desorption isotherm is used to calculate the pore volume as well as the average pore size of the distribution. The total surface area of the sample can be determined by the quantity of Nitrogen molecules obtained from the desorption-adsorption results together with pressure vibrations.

3. Results and Discussion

3.1. Fourier Transform Infrared Spectroscopic analysis (FTIR)

Figure 1 show the vibrational modes of FTIR spectra in treated HNT products which have been reported in previous HNT studies [21-24]. Table 3 lists the functional groups that have been determined by their wavelengths. The spectra of H0, H1, H3 and H8 in the O-H stretching of inner-surface hydroxyl group show similar absorption at 3692, 3694, 3694 and 3694 cm^{-1} respectively. Also, the spectra of H0, H1, H3 and H8 in the O-H stretching of inner hydroxyl group show similar spectra absorption at 3622, 3622, 3622 and 3621 cm^{-1}.

Figure 1

Another finding is that the group (O-H) was not evident for sample H21. The peak in the absorption of FTIR spectra occurs at 3547 cm^{-1} for O-H with intermolecular hydrogen group, but the O-H group was not evident for samples H1, H3, H8 and H21. The absorption for H1, H3, H8 and H21 are recoded at 2416, 3402, 3397 and 3388 respectively for O-H group with intermolecular hydrogen. However, there is no reading for H0 in this particular group with not found in H0. The samples; H0, H1, H3, H8 and H21 were also found in the C=C or Alkenyl group.

Table 3

2.1 X-ray diffraction (XRD)

The application of XRD is used mainly determine the structure of HNT with the purpose to show the enhancement of the HNT applications that have under gone the modification process

involving acid treatment [25, 26]. Figure 2 shows typical X-ray diffraction patterns of all natural halloysites (H0) and acid treated produced halloysites for various durations of treatment time. The diffraction peaks of natural halloysites (H0) and of after acid treatment was measured at the same angle of 2θ. The XRD is made up of a composition of H, halloysite; X, halloysite-(7 Å); M, sodium aluminium silicon oxide; S, quartz; R, silicon oxide and G, graphite for halloysite (H0) and acid treated halloysite. The findings reveal that the intensity peaks for acid treated samples show a decrease with increasing treatment time. This phenomenon of decreasing intensity is attributed to the agglomeration of HNT after acid treatment [25, 26]. This XRD results are supported and confirmed by the analysis of the results of FESEM and TEM.

Figure 2

3.2. TG-DTA data

Figure 3 (A & B) illustrate the TG-DTA curves of natural HNT and H_2SO_4 treated products. TG curves show two main stages of weight loss. The first stage that occurs at 30 ◦C and ends at 100 ◦C may be attributed to the dehydration of physisorbed water and interlayer water. The weight loss of natural HNT at this stage is higher than that of acid treated counterparts, whereby the weight loss may be attributed to the dehydration and destruction of HNT during H_2SO_4 treatment. The second stage occurs at 400 ◦C and ends at 550 ◦C, due to the dehydroxylation of structural water [12].

The weight loss of HNT shows decrease with longer duration of sulfuric acid treatment. The reason for this occurrence is that the structural hydroxyl groups in the AlO_6 octahedral layer are being removed alongside the dissolving of Al^{3+}. Meanwhile, the corresponding DTA curves of natural halloysite nanotubes and sulfuric acid treated products are consistent with that of TG results. The endothermic teaches a peak at 56.4–65.5 ◦C and 480.6–502.4 ◦C, respectively. It is found that all the samples are at endothermic status throughout the entire heating process. This has attributed to the continuous dehydration and dehydroxylation.

Figure 3 A and B

3.3. Morphology Characterization

3.3.1. FESEM and Mapping

Figure 4 shows the FESEM images of natural HNT (H0) before and after acid treatment. However, Figure 4 also shows the dispersion and distribution of the nanotubes together with their physical interaction. It was observed that there was a clear dispersion of HNT when of duration

stirring time was 3 hours. During this length of time, as the HNTs were homogeneously dispersed at a magnification of 100 K. The observations from the micrographs reveal that the individual nanotubes could not coerced together due to the presence of strong interfacial bonding between nanotubes. Another observation is the nanocomposites with higher HNT content showed obvious plastic deformation. This is caused strong reinforcing effects imparted by the HNT nanophase.

Figure 4

On the other hand, the EDS data of natural HNT recorded the atomic ratio of Si/Al as 1.13, which is almost the ideal value for HNT. Figure 5 shows the FESEM images of acid treated HNT for time duration of 1hr, 3hr, 8h and 21hr. The values of HNT composition were maintained under acid treatment time for 1h, 3h, 8h and 21h. This is because the sulfuric acid reacts with HNT at surface level. The EDS data of H1 reveals that the atomic ratio of Si/Al has increased to approximately 2, which is due to the dissolving of Al^{2+}.

Figure 5

3.4. BET surface area analysis

The analysis of N_2 adsorption-desorption are performed to investigate the surface area and pore volume of natural halloysite and acid treated halloysite. All the samples in Figure 6 display similar adsorption isotherms that are classified as type IV based on the recommendations by IUPAC. The samples are usually of mesoporous and microporous types [27].

Figure 6

Table 4 tabulates the values of BET surface area and pore volume of natural HNT and H_2SO_4 treated HNT. There is an increase in the BET surface area of HNT, from 59.04 m^2/g of H0 to 222.55 m^2/g of H1, before reaching a maximum of 306.43 m^2/g after for 8 h (H8) due to the dissolution of AlO_6 octahedral layers during H_2SO_4 treatment. Subsequently, the BET surface area of HNT decreases to 279.5 m^2/g (H21). This is attributed to the disaggregation of silica layers. It is also noted that the micropore volume of HNT changes slightly from 3 h to 8 h, due to the formation and blocking of micropores simultaneously [28]. It is found that the micropore fraction of treated HNT increases when the H_2SO_4 treating time is extended duration 1 to 8 hr, and when it is shortened at 21 hr.

The other finding reveals that the average pore size of HNT treated by H_2SO_4 shows an increase from 99.4 Å at 1 hr to 117.4 Å at 21 hr. Meanwhile, the average pore size of natural HNT

is of a much higher value, 167.3 Å, which is due to the opening of HNT. Figure 7 shows the distributions of micropore size of natural HNT and H_2SO_4 treated products. The distribution of SiO_4 tetrahedral and AlO_6 octahedral layers in halloysite shows a hierarchical formation. When H_2SO_4 treated time is increased from 1 to 21 hr. The distribution of the micropore size of HNT shows differences while the pore size and pore volume indicates an increase. The distribution of a fixed micropore size is to facilitate the utilization of acid treated HNT for various applications such as, drug supporters, enzyme carriers, and selective adsorbents.

Table 4

Figure 7

4. Conclusions

This study has investigated the enhancement of physical and chemical properties of HNTs using H_2SO_4 at various experimental conditions. It is observed that H_2SO_4 treatment break down the crystal structure of HNT before turning it into amorphous silica. Also, the FESEM images reveal H_2SO_4 treatment dissolves the AlO_6 octahedral layers and induces the disintegration of SiO_4 tetrahedral layers, resulting in porous nanorods. It is also found that the BET surface area and pore volume increases when the duration of H_2SO_4 treating time is extended duration 1 h to 8 h. Besides that, the micropores of obtained products are restricted by the crystalline structure due to the continuous H_2SO_4 treatment. Finally, the H_2SO_4 treated HNT has proven to be an effective low-cost adsorbent for its pH value is instrumental in the adsorption capacities.

Acknowledgments

The authors thank Universiti Kebangsaan Malaysia and the Ministry of Higher Education for the financial support grand DIP-2014-006 and LRGS/TD/2012/USM-UKM/PT/05.

Author Contributions

Tayser Sumer Gaaz was a PhD student and he did all the experiment as part of her project. Muneer Ba-Abbad was help in characterization of the nanomaterial. Abu Bakar Sulong and Abdul Amir H. Kadhum were the principle investigators while Ahmed A. Al-Amiery was co-investigators. All authors are aware of this manuscript and have agreed to its publication.

Conflicts of Interest

The authors declare no conflict of interest.

References

1. García, F.J., et al., *Study of natural halloysite from the Dragon Mine, Utah (USA).* Zeitschrift für anorganische und allgemeine Chemie, 2009. **635**(4-5): p. 790-795.
2. Ece, Ö.I. and P.A. Schroeder, *Clay mineralogy and chemistry of halloysite and alunite deposits in the Turplu area, Balikesir, Turkey.* Clays and Clay Minerals, 2007. **55**(1): p. 18-35.
3. Singer, A., et al., *Halloysite characteristics and formation in the northern Golan Heights.* Geoderma, 2004. **123**(3): p. 279-295.
4. Joussein, E., et al., *Halloysite clay minerals—a review.* Clay Minerals, 2005. **40**(4): p. 383-426.
5. Kautz, C.Q. and P.C. Ryan, *The 10 Å to 7 Å halloysite transition in a tropical soil sequence, Costa Rica.* Clays and Clay Minerals, 2003. **51**(3): p. 252-263.
6. Lvov, Y., et al., *Thin film nanofabrication via layer-by-layer adsorption of tubule halloysite, spherical silica, proteins and polycations.* Colloids and Surfaces A: Physicochemical and Engineering Aspects, 2002. **198**: p. 375-382.
7. Du, M., B. Guo, and D. Jia, *Newly emerging applications of halloysite nanotubes: a review.* Polymer International, 2010. **59**(5): p. 574-582.
8. Belver, C., M.A. Bañares Muñoz, and M.A. Vicente, *Chemical activation of a kaolinite under acid and alkaline conditions.* Chemistry of materials, 2002. **14**(5): p. 2033-2043.
9. Frini-Srasra, N. and E. Srasra, *Effect of heating on palygorskite and acid treated palygorskite properties.* Surface Engineering and Applied Electrochemistry, 2008. **44**(1): p. 43-49.
10. Kennedy Oubagaranadin, J.U. and Z. Murthy, *Characterization and use of acid-activated montmorillonite-illite type of clay for lead (II) removal.* AIChE journal, 2010. **56**(9): p. 2312-2322.
11. Zhang, J., et al., *XRF and nitrogen adsorption studies of acid-activated palygorskite.* Clay Minerals, 2010. **45**(2): p. 145-156.
12. Panda, A.K., et al., *Effect of sulphuric acid treatment on the physico-chemical characteristics of kaolin clay.* Colloids and Surfaces A: Physicochemical and Engineering Aspects, 2010. **363**(1): p. 98-104.
13. Swapna, V., et al., *Thermal properties of poly (vinyl alcohol)(PVA)/halloysite nanotubes reinforced nanocomposites.* International Journal of Plastics Technology, 2015: p. 1-13.
14. Lenarda, M., et al., *Solid acid catalysts from clays: preparation of mesoporous catalysts by chemical activation of metakaolin under acid conditions.* Journal of colloid and interface science, 2007. **311**(2): p. 537-543.

15. Levis, S. and P. Deasy, *Characterisation of halloysite for use as a microtubular drug delivery system.* International Journal of Pharmaceutics, 2002. **243**(1): p. 125-134.
16. Jinhua, W., et al., *Rapid adsorption of Cr (VI) on modified halloysite nanotubes.* Desalination, 2010. **259**(1): p. 22-28.
17. Zhao, M. and P. Liu, *Adsorption behavior of methylene blue on halloysite nanotubes.* Microporous and Mesoporous Materials, 2008. **112**(1): p. 419-424.
18. Liu, S., et al., *Preformed zeolite precursor route for synthesis of mesoporous X zeolite.* Colloids and Surfaces A: Physicochemical and Engineering Aspects, 2008. **318**(1): p. 269-274.
19. Liu, R., et al., *Adsorption of methyl violet from aqueous solution by halloysite nanotubes.* Desalination, 2011. **268**(1): p. 111-116.
20. Wang, Q., et al., *Adsorption and release of ofloxacin from acid-and heat-treated halloysite.* Colloids and Surfaces B: Biointerfaces, 2014. **113**: p. 51-58.
21. Frost, R.L. and A.M. Vassallo, *The dehydroxylation of the kaolinite clay minerals using infrared emission spectroscopy.* Clays and Clay Minerals, 1996. **44**(5): p. 635-651.
22. Morterra, C. and G. Magnacca, *A case study: surface chemistry and surface structure of catalytic aluminas, as studied by vibrational spectroscopy of adsorbed species.* Catalysis Today, 1996. **27**(3): p. 497-532.
23. Koretsky, C.M., et al., *Detection of surface hydroxyl species on quartz, γ-alumina, and feldspars using diffuse reflectance infrared spectroscopy.* Geochimica et Cosmochimica Acta, 1997. **61**(11): p. 2193-2210.
24. Madejová, J. and P. Komadel, *Baseline studies of the clay minerals society source clays: infrared methods.* Clays and clay minerals, 2001. **49**(5): p. 410-432.
25. Ba-Abbad, M.M., et al., *Visible light photocatalytic activity of Fe 3+-doped ZnO nanoparticle prepared via sol–gel technique.* Chemosphere, 2013. **91**(11): p. 1604-1611.
26. Ba-Abbad, M.M., et al., *The effect of process parameters on the size of ZnO nanoparticles synthesized via the sol–gel technique.* Journal of Alloys and Compounds, 2013. **550**: p. 63-70.
27. Papoulis, D., et al., *Palygorskite-and Halloysite-TiO_2 nanocomposites: Synthesis and photocatalytic activity.* Applied Clay Science, 2010. **50**(1): p. 118-124.
28. Chen, X.-G., et al., *Thermal destruction of rice hull in air and nitrogen.* Journal of thermal analysis and calorimetry, 2011. **104**(3): p. 1055-1062.
29. Zhang, A.-B., et al., *Effects of acid treatment on the physico-chemical and pore characteristics of halloysite.* Colloids and Surfaces A: Physicochemical and Engineering Aspects, 2012. **396**: p. 182-188.

Figure 1. FTIR pattern of natural HNT (H0) and H_2SO_4 treated products as a function of H_2SO_4 treatment durations (H1–H21, the numbers represent the duration of H_2SO_4 treatment durations).

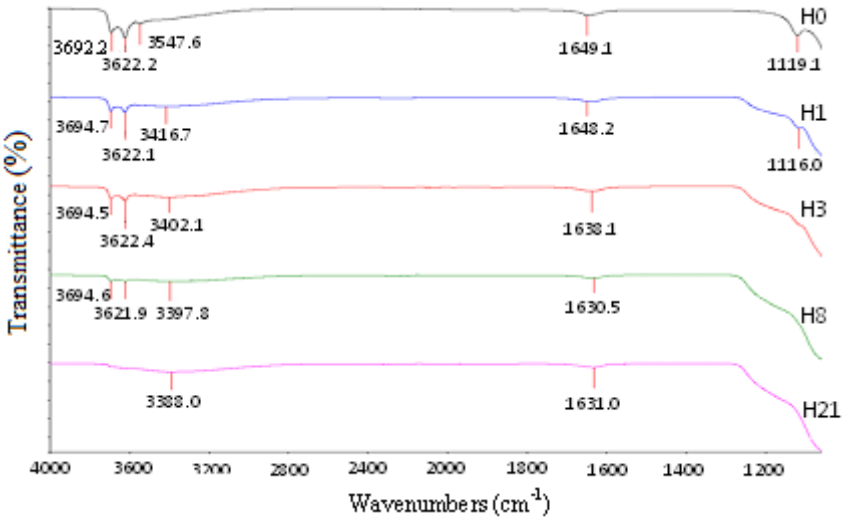

Figure 2 XRD patterns of natural HNT (H0) and of H_2SO_4 treated products as a function of the duration of H_2SO_4 treatment (H1–H21, the numbers represent the time duration for each H_2SO_4 treatment): H, halloysite ; X, halloysite-(7 Å); M, sodium aluminium silicon oxide; S, quartz; R, silicon oxide; G, graphite.

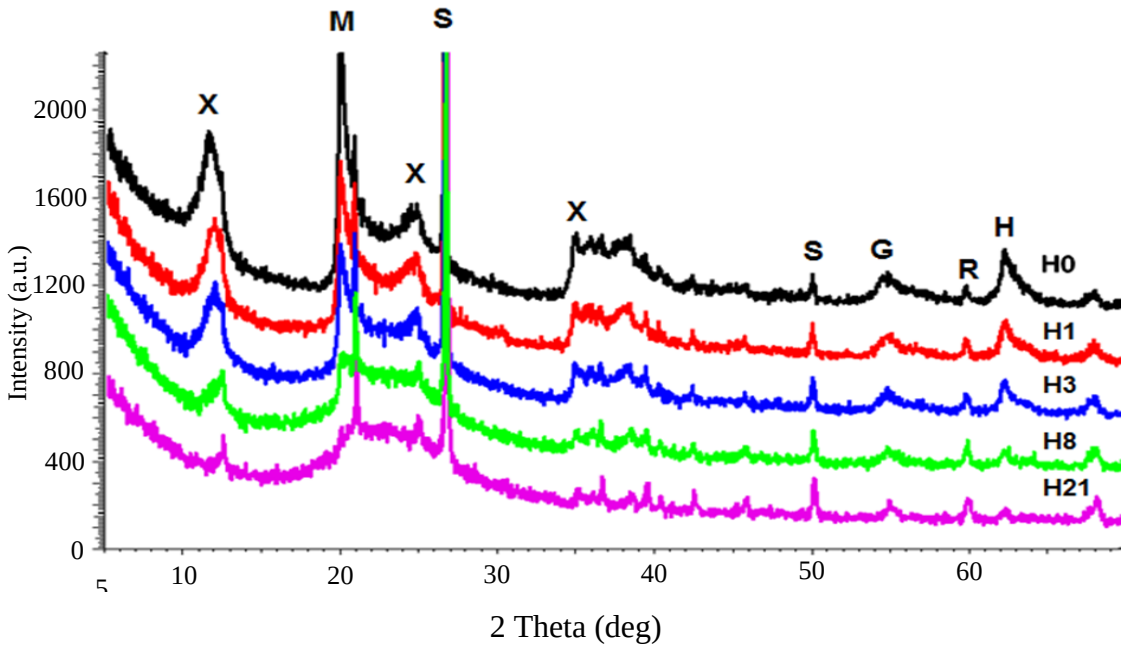

Figure 3 A. TGA curves of natural HNT (H0) and H_2SO_4 treated products as a function of the durations of H_2SO_4 treatment (H1–H21, the numbers represent the duration of each H_2SO_4 treatment).

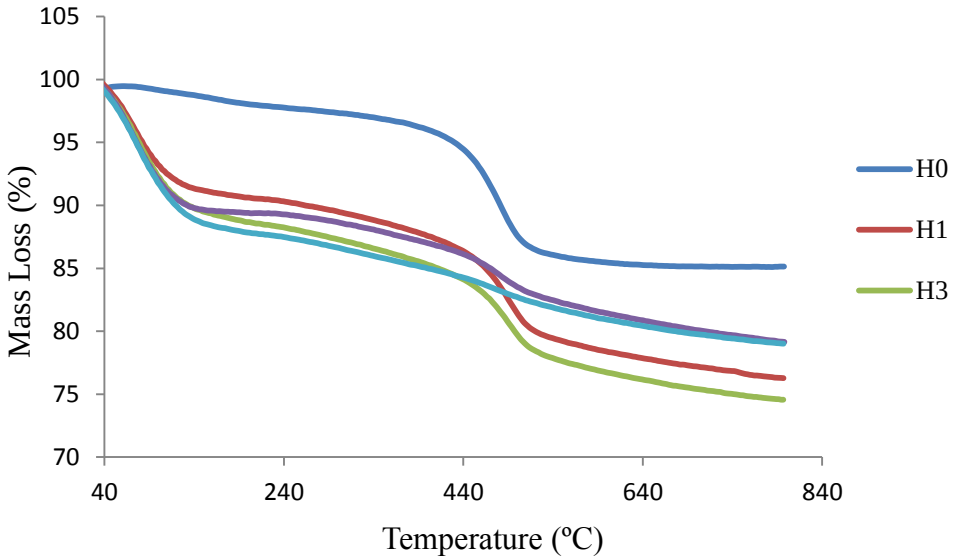

Figure 3 B. DTA curves of natural HNT (H0) and H_2SO_4 treated products as a function of the durations of H_2SO_4 treatment (H1–H21, the numbers represent the duration of each H_2SO_4 treatment).

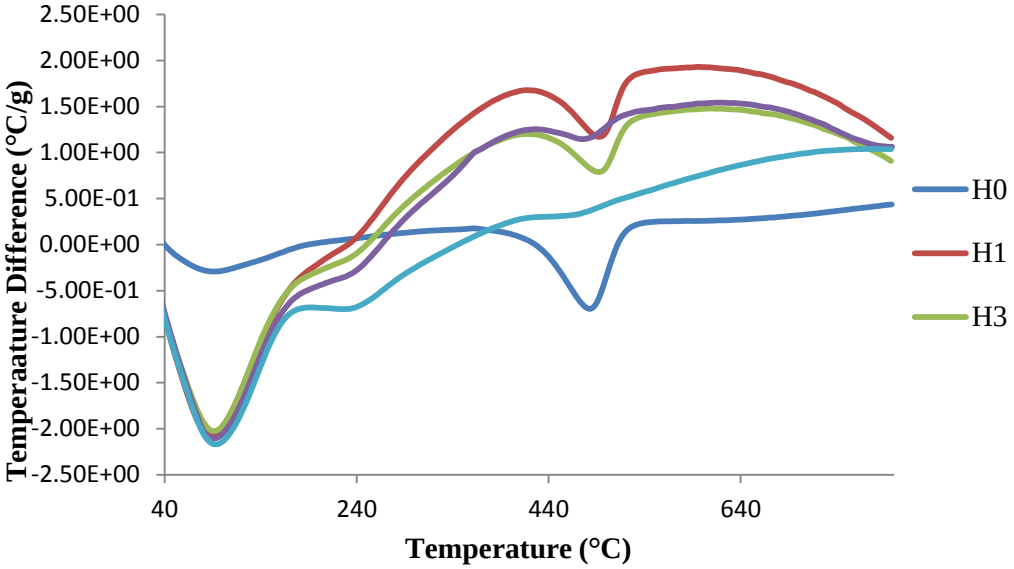

Figure 4 FESEM microphotographs for: (a) (H0) Neat HNT, (b) H1 (1 hour), (c) H3 (3 hour), (d) H8 (8 hour) and (e) H21 (21 hour) at a magnification of 100.00 KX.

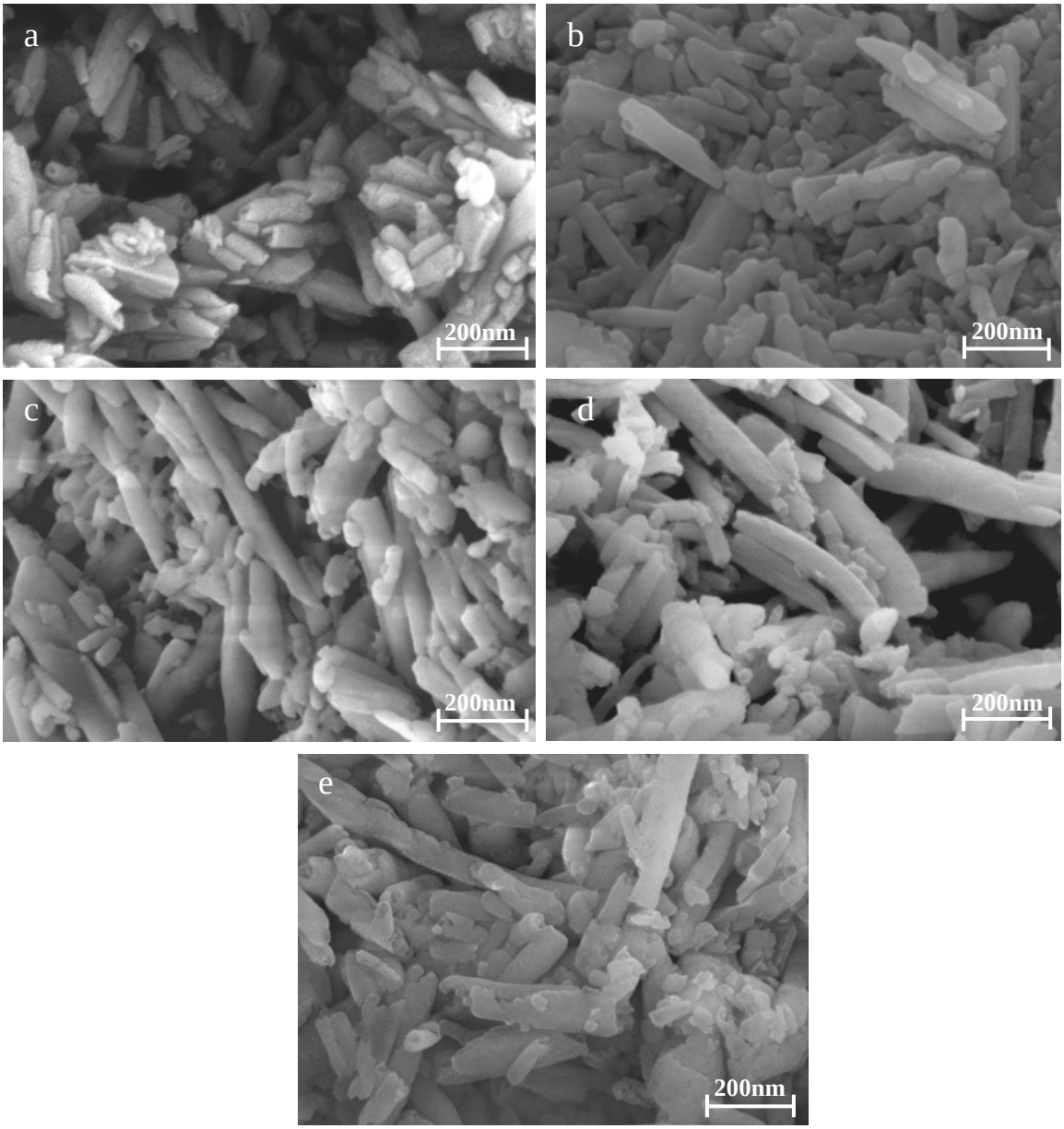

Figure 5 Mapping and EDX for: (a) (H0) Neat HNT , (b) H1 (1 hour), (c) H3 (3 hour), (d) H8 (8 hour) and (e) H21 (21 hour).

(a)

Element	Weight%	Atomic%
O K	59.59	71.76
Al K	18.54	13.24
Si K	21.87	15.00

(b)

Element	Weight%	Atomic%
O K	54.24	67.25
Al K	14.84	10.91
Si K	30.93	21.84

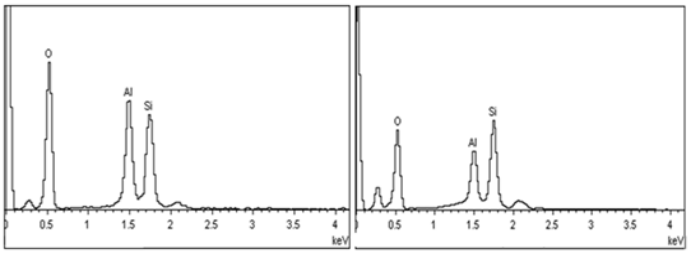

(c)

Element	Weight%	Atomic%
O K	57.18	69.77
Al K	16.18	11.71
Si K	26.64	18.52

(d)

Element	Weight%	Atomic%
O	60.76	72.98
Al	6.40	4.56

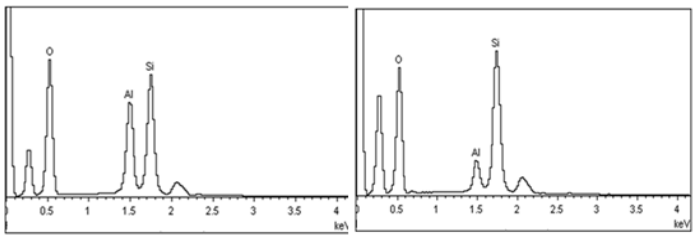

(e)

Element	Weight%	Atomic%
O	55.28	68.43
Al	0.91	0.67
Si	43.81	30.90

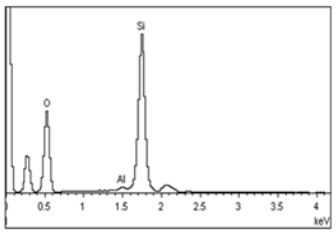

Figure 6 N_2 adsorption-desorption curves of natural HNT (H0) and H_2SO_4 treated products as a function of the durations of H_2SO_4 treatment (H1–H21, the numbers represent the durations of H_2SO_4 treatment).

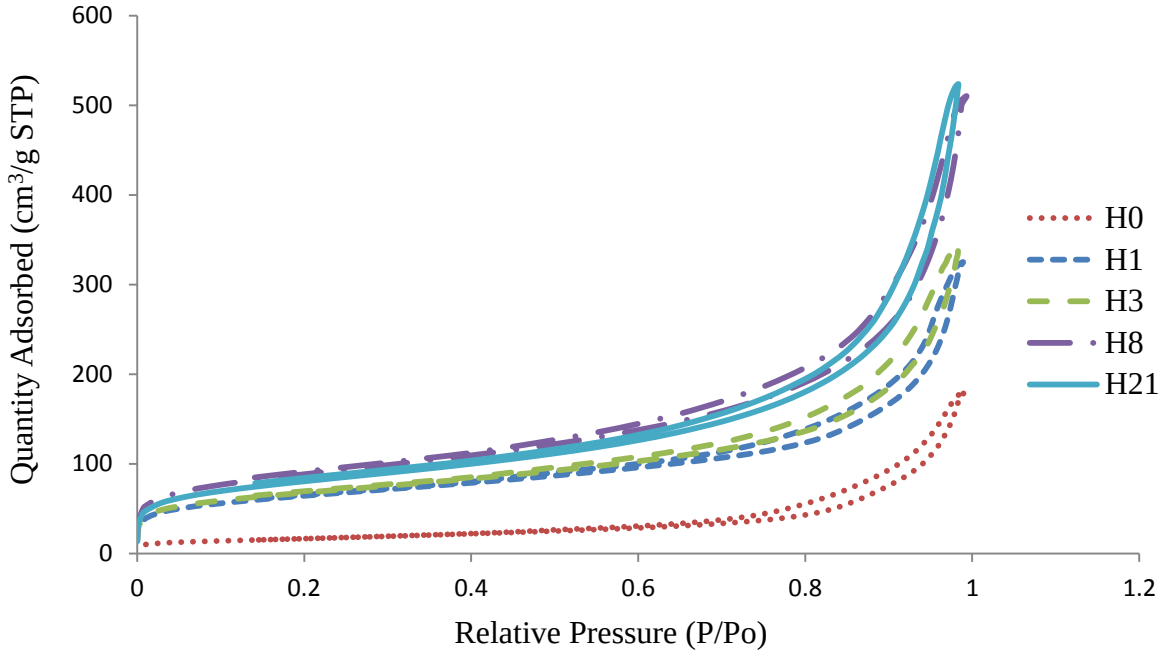

Figure 7 Distribution micropore size of natural HNT (H0) and H_2SO_4 treated products as a function of the durations of H_2SO_4 treatment (H1–H21, the numbers represent the durations of H_2SO_4 treatment).

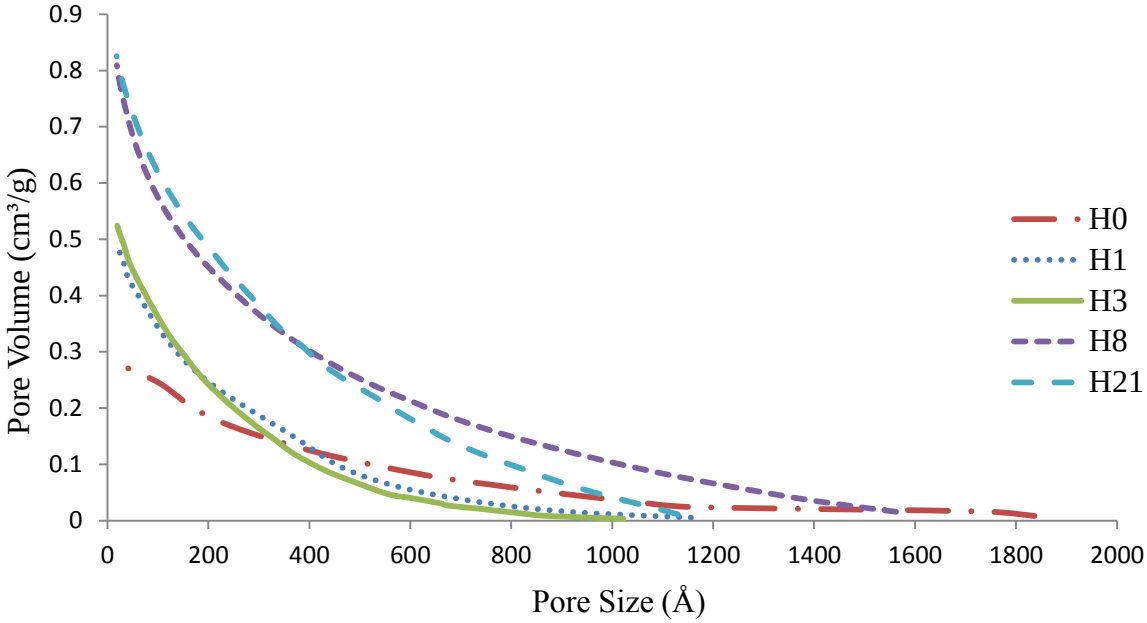

Table 1 Chemical compositions of HNT

Chemical compositions	SiO_2	Al_2O_3	Fe_2O_3	MgO	TiO_2
Weight %	61.19	18.11	0.49	0.10	20.11

Table 2 Physical properties of HNT

Typical analysis of natural HNT	
Chemistry	$Al_2Si_2O_5(OH)_4.nH_2O$
d50(median particle size)	1.0 μ
Aspect ratio (L/D)	~15
Surface area (BET)	65 m^2/g
Specific gravity	2.54 g/cm^3
Refractive Index	1.54

Table 3. Positions and assignments of the IR vibration bands.

Position (cm^{-1})	Assignments
3992	O-H stretching of inner-surface hydroxyl group
3994	O-H stretching of inner-surface hydroxyl group
3622	O-H stretching of inner hydroxyl group
3621	O-H stretching of inner hydroxyl group
3547	O-H with intermolecular hydrogen group
3388 – 3416	O-H with intermolecular hydrogen group

Table 4 Surface areas and pore volumes of natural halloysite and H_2SO_4 treated halloysite.

HNT	S_{BET} (m^2/g)	Total pore volume (cm^3/g)	Micropore volume (cm^3/g)	S_{ads} of pores (17.0 Å and 3000.0 Å diameter) (m^2/g)	V_{ads} of pores (17.0 Å- 3000.0 Å diameter) (cm^3/g)	Average pore size Å	S_{BET} (m^2/g) reported by others*
H0	59.04	0.26	0.001	67.99	0.28	167.3	47.8
H1	222.55	0.45	0.018	199.66	0.49	99.4	207.6
H3	234.53	0.48	0.019	215.01	0.52	98.4	259.1
H8	306.43	0.71	0.022	303.57	0.81	106.6	248.4
H21	279.47	0.74	0.018	281.16	0.82	117.4	134.1

*Zhang et al. [29]